Seismic response analysis of the tunnel with accumulated damage and crack effect in shaking table test

Z.Z. Wang [1], B. Gao [1], T.C. Sun [1, 2], Y.S. Shen [1]

[1] *School of Civil Engineering, Southwest Jiaotong University , Chengdu, China*
[2] *Dept. of Civil Engineering, Shijiazhuang Railway College, Shijiazhuang, China*
Email: ipod2prince@yahoo.com.cn

ABSTRACT :

Based on the background of tunnels to be constructed on high seismic intensity zone in southwest China, the large-scale shaking table test was conducted for studying the seismic capability of the tunnel portal structure. The aim of this paper is three-part: (a) to provide details of a series of shaking table experiments, (b) to understand the failure behavior at the certain excitation, and (c) to demonstrate that the response of these experiments can be simulated accurately under the damage-plastic model of geotechnical materials. The conclusion of this study should be of interest and use to professionals involved in the design of tunnel portal structures.

KEYWORDS: accumulated damage; crack effects; tunnel portal; seismic response; shaking table test

1. INTRODUCTION

Tunnels built in areas subject to earthquake activity must withstand both seismic and static loading. Historically, tunnels have experienced a lower rate of damage than surface structures. Nevertheless, some tunnels have experienced significant damage in recent large earthquakes, including the 1995 Kobe, Japan earthquake, the 1999 Chi-Chi, Taiwan earthquake and the 1999 Kocaeli, Turkey earthquake.

Several studies have documented earthquake damage to underground facilities. ASCE (1974) describes the damage in the Los Angeles area as a result of the 1971 San Fernando Earthquake. JSCE (1988) describes the performance of several underground structures, including an immersed tube tunnel during shaking in Japan. Duke and Leeds (1959), Stevens (1977), Dowding and Rozen (1978), Owen and Scholl (1981) and Kaneshiro et al. (2000), all present summaries of case histories of damage to underground facilities.

On the basis of the background of tunnels to be constructed on high seismic intensity zone in southwest China, the seismic response of the tunnel portal structure is analyzed and presented in this paper. Large-scale shaking table tests were conducted for studying the seismic capability of the tunnel portal structure. Meanwhile, a three-dimensional model is established and dynamic analysis is conducted numerically. The aim of this paper is three-part: (a) to provide details of a series of shaking table experiments, (b) to understand the failure behavior at the certain excitation, and (c) to demonstrate that the response of these experiments can be simulated accurately under the damage-plastic model of geotechnical materials The conclusion of this study should be of interest and use to professionals involved in the design of tunnel portal structures.

2. THE SHAKING TABLE TEST

2.1 Shaking Table and model box

The shaking table at the Traction Power State Key Laboratory is the main facility for experimental research into earthquake engineering at Southwest Jiaotong University. It consists of a 3m by 3m platform capable of carrying a maximum payload of 80t. It is driven horizontally and vertically by four 20kN servo actuators giving full control of motion of the platform in 4 DOF simultaneously.

In the test, the model box was fastened to the shaking table, and the seismic accelerograms were input into the control device of the shaking table. The shaking table vibrated according to the input seismic records, simulating the earthquake excitations on the ground. Measurements were made to obtain the responses of acceleration and strain at the critical location. The measurement system and arrangement of the equipment are shown in Fig. 1

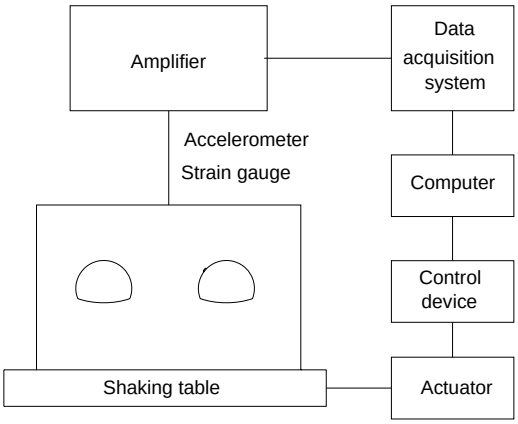

Fig. 1 Measurement system of the model test

2.3 Sensors Layout

The sensors used in shaking table tests include accelerometers and strain gauges. On the basis of the previous seismic damage experience with tunnels and the 3D numerical analysis of the model under the same conditions, the locations of accelerometers and strain gauges were determined for the present model test. Accelerometers were mainly installed at the crown, shoulder, spring and invert of the tunnel, while the strain gauges were mainly distributed on the soil, and at the invert of the tunnel. The layout of the measuring points is shown is Fig. 2.

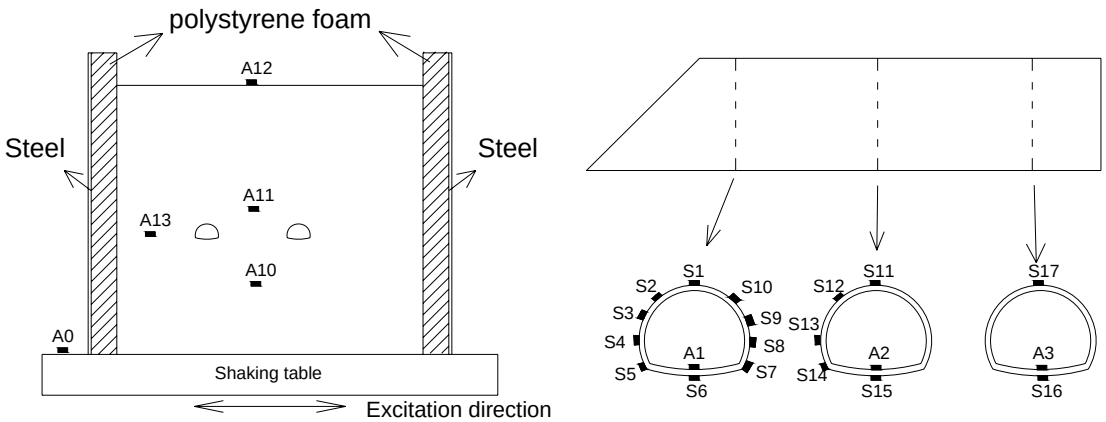

Fig. 2 Layout scheme of sensors

2.4 Input Earthquake

According to the previously stated requirements and other site conditions information in the tunnel area, one artificial earthquake accelerogram (shown in Fig. 3) produced by the Sichuan Sast Tech. Co. Ltd was adopted in the shaking table test. Based on the similitude law (Hirama et al., 2005a) for the test model, the time axis of the input earthquake waveform was obtained by reducing the real earthquake by a factor of 1/5.5.

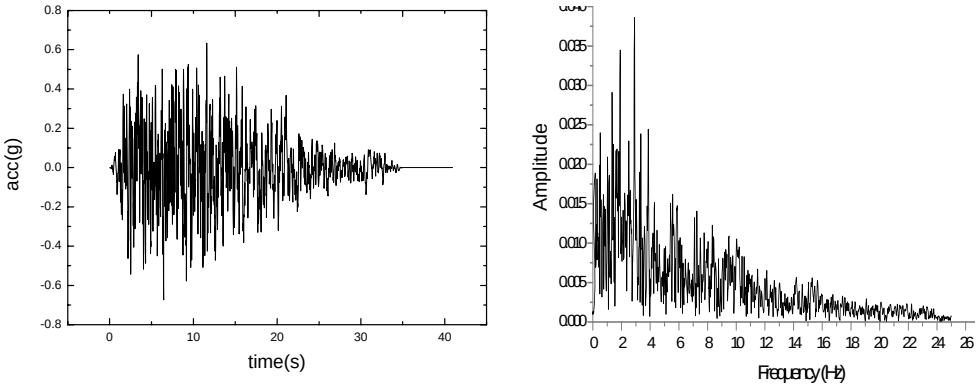

Fig. 3 Artificial waveform adopted in shaking table tests and its Fourier spectrum

2.5 Loading Scheme

The experimental system was excited by two waveforms. First, a low-amplitude (0.05g), broadband (0~50Hz) white-noise excitation was used to explore the frequency response of the model system. Then, an appropriately scaled artificial earthquake motion was input. The input acceleration increased from 0.14~0.78g, shown in table 1. The white-noise excitation is also designed to obtain natural responses of the model system after every earthquake excitation. The purpose of white-noise excitation is to recognize the damage of the model system after every earthquake excitation.

Table 1 Loading scheme

Loading number	Waveform	Acceleration peak	Test content
1	White noise	0.05g	Frequency property
2	Artificial wave	0.14g	Dynamic damage response
3	White noise	0.05g	Frequency property
4	Artificial wave	0.22g	Dynamic damage response
5	White noise	0.05g	Frequency property
6	Artificial wave	0.31g	dynamic damage response
7	White noise	0.05g	Frequency property
8	Artificial wave	0.42g	dynamic damage response
9	White noise	0.05g	Frequency property
10	Artificial wave	0.54g	dynamic damage response
11	White noise	0.05g	Frequency property
12	Artificial wave	0.78g	dynamic damage response
13	White noise	0.05g	Frequency property

2.6 Test Results And Analysis

2.6.1 Behavior of test model up to 0.31g

Table 2 shows the acceleration responses at critical locations of the model. From table 2, it can be observed that the acceleration magnification factors gradually increase from the inner to near the tunnel portal. This is because the restriction of the portal is relatively weak.

Table 2 Dynamic magnification factor at critical locations of the model

Critical location of the model*	A1	A2	A3	A10	A11	A12
Dynamic magnification factor	1.43	1.35	1.31	1.13	1.28	1.37

*critical locations of the model are shown in Fig. 2

The dynamic strain responses at some critical locations are shown in Fig. 4.

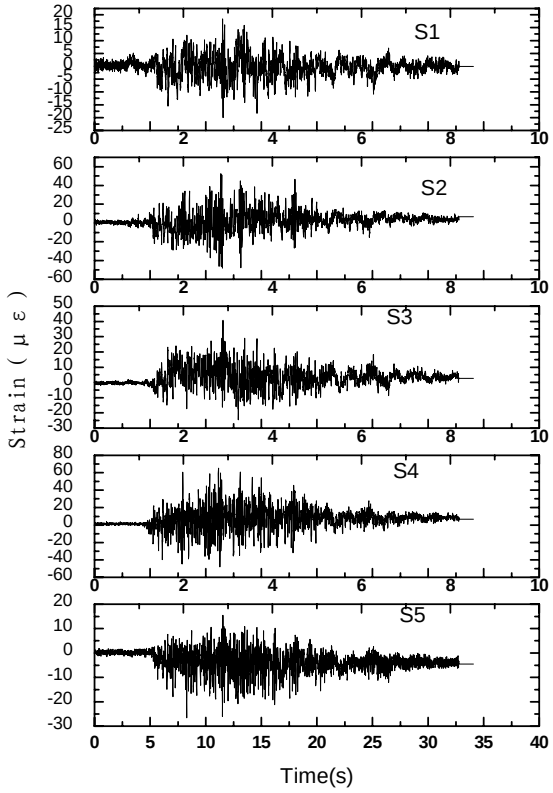

Fig. 4 Strain time histories at some critical locations (critical locations are shown in Fig. 2)

From Fig.4, it can be observed that the dynamic strain is relatively large at the foot of the tunnel, about 6.0×10^{-5}. This is due to the fact that the stress concentration is inclined to occur at that location. So it can be concluded that the foot is the weakest location in the cross-section of the tunnel.

2.6.2 Behavior of test model at final excitation (0.78g)

After the elastic test was conducted, the destruction test of the tunnel model was carried out. In the destruction test, the acceleration of the shaking table was gradually increased until the model was totally destroyed. This section describes the behavior and failure mode for the period up to test model failure at the final excitation of 0.78g.

The frequency response of the model system is obtained by white-noise excitation and the result is displayed in Fig. 5. Fig.5 shows the changes in the natural frequency of the model system was not obvious when the peak acceleration increased from 0.14~0.31g. But the frequency decreased sharply after the acceleration peak reached 0.42g. It can be concluded that the model system initiated to damage under the acceleration of 0.42g.

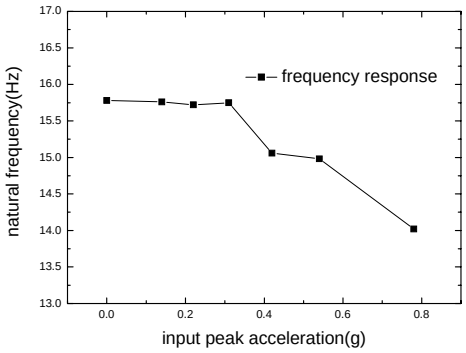

Fig. 5 Natural frequency response of the model system at white-noise excitation

Fig. 6 shows the failure progress of the test model. It can be observed that some cracks appear at the crown, shoulder, and foot of the tunnel as the peak acceleration reached 0.42g, The model was fully destroyed as the peak acceleration reached 0.78g.

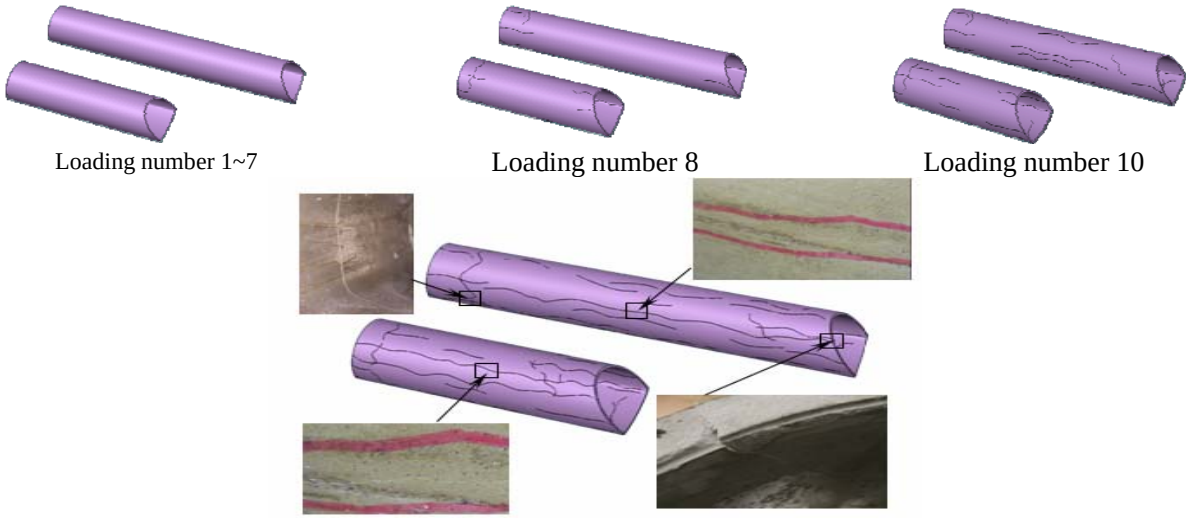

Fig. 6 Crack distribution on damaged lining

Fig. 7 shows the crack expansion routes on the model soil. Two main cracks appeared at the surface of the model slope, starting from the interface between model tunnel and model soil, mainly due to the dynamic interaction between the two.

From Fig. 6 and Fig.7, it can be concluded that damage at and near tunnel portals is significant due to slope instability. The only technically feasible way to mitigate slope instability is to stabilize the ground.

Fig. 7 Crack distribution on damaged soil after final excitation

3. NUMERICAL ANALYSIS

3.1 Dynamic Damage Equation

The dynamic damage finite element equation is given in Eq. (3.1).

$$M\ddot{u} + C(d)\dot{u} + K(d)u = P(t) \tag{3.1}$$

Where d stands for the damage variable and M, C(d), and D(d) are the mass, damping, and stiffness matrices, respectively.

The Newmark method is applied to the time discretization of the Eq. (3.1), so the iteration algorithm of incremental displacement can be written as Eq. (3.2).

$$\tilde{K}\,\Delta u^{k}_{t+\Delta t} = f_{t+\Delta t} - p^{k}_{t+\Delta t} - [\frac{4}{\Delta t^{2}}M + \frac{2}{\Delta t}C]u^{k}_{t+\Delta t} + [\frac{4}{\Delta t^{2}}M + \frac{2}{\Delta t}C]u_{t} + M\ddot{u}_{t} \tag{3.2}$$

Where:

$$\tilde{K} = K + \frac{4}{\Delta t^{2}}M + \frac{2}{\Delta t}C \tag{3.3}$$

$$\Delta u^{k}_{t+\Delta t} = u^{k+1}_{t+\Delta t} - u^{k}_{t+\Delta t} \tag{3.4}$$

$$p^{k}_{t+\Delta t} = Ku^{k}_{t+\Delta t} \tag{3.5}$$

Where $f_{t+\Delta t}$ stands for the earthquake load at time $t+\Delta t$.
The convergence criterion is based on the ratio of nonequilibrium force norm to incremental force norm.

3.2 damage-plastic Model

The damage-plastic model is adopted in the numerical analysis. The stress-strain relations are governed by scalar damaged elasticity:

$$\sigma = (1-d)D^{el}_{0} : (\varepsilon - \varepsilon^{pl}) = D^{el} : (\varepsilon - \varepsilon^{pl})$$

Where D^{el}_{0} is the initial (undamaged) elastic stiffness of the material;
$D^{el} = (1-d)D^{el}_{0}$ is the degraded elastic stiffness; and *d* is the scalar stiffness degradation variable, which can take values in the range from zero (undamaged material) to one (fully damaged material). Damage associated with the failure mechanisms of the geotechnical materials (cracking and crushing) therefore results in a reduction in the elastic stiffness.

3.3 numerical model

The numerical model is shown in Fig. 8. The parameters, the boundary conditions, and the input seismic waveform adopted in the numerical analysis are the same as those in shaking table test.

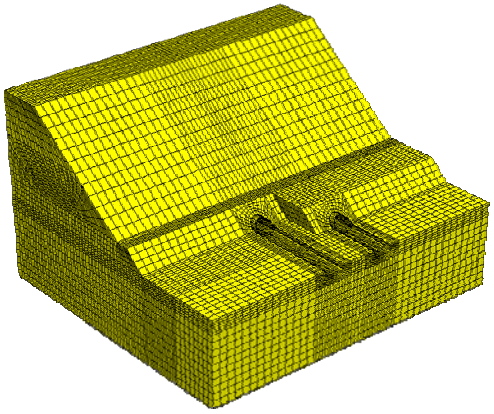

Fig.8 Numerical model

3.4 Results And Discussion

Detailed results are referred in another paper (Z.Z. Wang, et al., to be published later). Some results obtained from the numerical simulation are shown in table 3 and Fig. 9.

Table 3 The comparison of dynamic magnification factor between test and numerical simulation

Critical location	Dynamic magnification factor	
	Test	Calculated
A1	1.43	1.51
A2	1.35	1.38
A3	1.31	1.29
A10	1.13	1.17
A11	1.28	1.22
A12	1.37	1.41

From table 3, it can be concluded that the calculated dynamic magnification factors and those obtained from the model test are very close, and thus the accuracy of the numerical simulation is verified.

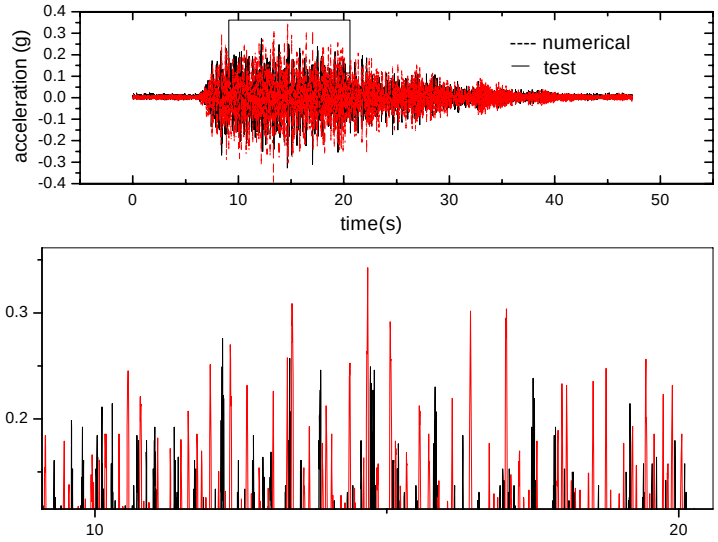

Fig. 9 calculated (dashed line) and measured (solid line) response at the invert of the tunnel

Fig. 9 shows the calculated (dashed line) and measured (solid line) response at the invert (A1) of the tunnel.

The calculated acceleration presents minor differences in the amplitude from the one obtained from the shaking table test, mainly due to the inadequacy in considering the material damping. Overall, the numerical simulations adequately reproduce the response of the model in shaking table test.

4. CONCLUSION

The main objective of the work presented in this paper is to study the seismic behavior of the tunnel to be built on high seismic intensity zone in southwest China. A combined experimental and numerical study on the seismic responses of the tunnel portal prosper a better understanding of the damage pattern and led to the following conclusions:

(1) The tunnel studied in this paper has a relatively high seismic capability and could guarantee the safety under the seismic action with the fortification intensity of 8 degree, as defined in the seismic design code of China.

(2) The seismic response of tunnels should take the accumulated damage and crack effect into consideration.

(3) Damage at and near tunnel portals is significant due to slope instability. The only technically feasible way to mitigate slope instability is to stabilize the ground.

Acknowledgements

This study was performed in the framework of the Sichuan commutation department science and technology project entitled *earthquake-resistance and mitigation measurements study of tunnels on high seismic intensity zone* (Contract No. 2006A24-58). The work described in this paper was partially supported by Southwest Jiaotong University doctoral students' innovation fund. The authors deeply acknowledge their contribution to the scientific supervision of the study.

REFERENCES

Chen G.X., Zhuang H.Y., Du X.L. (2007). Large-size shaking table test on soil-underground structure interaction. Earthquake Engineering and Engineering Vibration 27(2), 171-176.

Dimitris Pitilakis, Matt Dietz, David Muir Wood. (2007). Numerical simulation of dynamic soil-structure in shaking table testing. Soil Dynamics and Earthquake Engineering 10.1016.

Dowding C.H., Rozen A. (1978). Damage to rock tunnels from earthquake shaking. Journal of the Geotechnical Engineering Division. ASCE(GT2), 175-191.

JSCE, (1988). Earthquake Resistant Design for Civil Engineering Structures in Japan. Japanese Society of Civil Engineer, Tokyo.

Q.S. Li, Z.N. Li, G.Q. Li. (2005). Experimental and numerical seismic investigations of the Three Gorges dam. Engineering Structures 27(2005), 501-513.

Sharma, Willian R.J., Lei Qianrong. (1992). Damage of earthquake to underground hole. Underground Space 12(4), 335-344.

Toshihiko Hirama, Massashi Goto, Keiji Shiba, Toshio Kobayashi. (2005). Seismic proof test of a reinforced concrete containment vessel (RCCV). Nuclear Engineering and Design 235(2005), 1349-1371.

Ueng T.S., M.L., Chen M.H. (2001). Some geotechnical aspects of 1999 Chi-Chi, Taiwan earthquake. Proceedings of the Fourth International Conference on Recent Advances in Geotechnical Earthquake Engineering and Soil Dynamics. SPL-10.1,5.

Youssef M.A. Hashash, Jeffrey J. Hook, and Birger Schmidt. (2001). Seismic design and analysis of underground structures. Tunnelling and Underground Space Technology 16, 247-293.

Yang L.D., Ji Q.Q., Zheng Y.L. (2003). Shaking table tests on metro structures. Modern Tunneling Technology 40(1), 7-11.